BCG Vaccine Efficacy against *Mycobacterium tuberculosis* is Enhanced by the Alveolar Lining Fluid of the Lung

Juan I. Moliva[1,2], Austin P. Hossfeld[1], Cynthia H. Canan[1,2], Varun Dwivedi[1], Mark D. Wewers[3], Gillian Beamer[4], Joanne Turner[1,*], and Jordi B. Torrelles[1,*]

[1]Department of Microbial Infection and Immunity, College of Medicine, The Ohio State University, Columbus, Ohio 43210, USA; [2]Biomedical Sciences Graduate Program, College of Medicine, The Ohio State University, Columbus, Ohio 43210, USA; [3]Department of Internal Medicine, Pulmonary, Critical Care and Sleep Medicine Division, College of Medicine, The Ohio State University, Columbus, OH 43210, USA; [4]Department of Infectious Diseases and Global Health, Cummings School of Veterinary Medicine, Tufts University, North Grafton, MA 01536 USA.

*__Corresponding authors__: Dr. Joanne Turner, The Ohio State University (OSU), Department of Microbial Infection and Immunity, Biomedical Research Tower (BRT), Room 786, 460 W. 12th Ave, , Columbus, OH, 43210, phone: 614-292-6724; fax: 614-292-9616; Email: joanne.turner@osumc.edu; and Dr. Jordi B. Torrelles, OSU, Department of Microbial Infection and Immunity, BRT, Room 708, 460 W. 12th Ave, Columbus, OH, 43210; phone: 614-292-0777; fax: 614-292-9616; Email: jordi.torrelles@osumc.edu

Keywords: Tuberculosis, *Mycobacterium tuberculosis*, BCG vaccine, lung immunology, CD8 T-cell

ABSTRACT

Few studies have considered the impact of the human lung environment in tuberculosis vaccination design. However, we have shown that exposure of *Mycobacterium tuberculosis* (*M.tb*) to human lung mucosa [alveolar lining fluid (ALF)] modifies the *M.tb* cell wall, revealing alternate antigenic epitopes on the bacterium surface that effect its pathogenicity. Here we vaccinated mice with ALF-exposed BCG, mimicking the mycobacterial cell surface properties that would be present in the lung during *M.tb* infection. ALF-exposed BCG vaccinated mice were more effective at reducing *M.tb* bacterial burden in the lung and spleen, and had reduced lung inflammation at late stages of *M.tb* infection. Improved BCG efficacy was associated with and dependent on increased numbers of memory and IFNγ secreting $CD8^+$ T-cells in the lung in response to *M.tb* challenge. We conclude that ALF modifications to the *M.tb* cell wall *in vivo* are relevant in the context of vaccine design.

Tuberculosis (TB) is now the leading cause of death attributed to a single infectious organism[1]. *Mycobacterium bovis* Bacille de Calmette *et* Guérin (BCG) is the only vaccine currently supported by the World Health Organization for the prevention of TB. However, BCG efficacy at preventing TB is highly variable[2, 3], and its protective immunity appears to last for 10-15 years[4].

During the natural course of infection with *Mycobacterium tuberculosis* (*M.tb*), bacilli are inhaled and deposited in the alveolar sacs of the lung[5] where they are bathed in alveolar lining fluid (ALF)[6]. In this study we hypothesized that ALF modification of BCG would induce better protection against aerosol infection with *M.tb.* We based our hypothesis on the fact that 1) The majority of *M.tb* infection is established via the lung[7]; 2) deposition of *M.tb* bacilli in the alveolar space results in exposure to ALF[8]; 3) exposure to ALF alters the cell wall of *M.tb* revealing new antigenic motifs on the surface of the bacillus[8], with consequences in uptake and phagocytosis by phagocytes[8-10]; and 4) this *M.tb*-ALF interaction occurs prior to the development of cellular immunity against *M.tb* infection. As a result, we postulated that cellular innate and adaptive immune responses in the lung would be generated in response to an 'ALF-modified *M.tb*', a phenomenon that could affect the efficacy of BCG vaccination. Here we demonstrate that changes on the BCG cell wall surface, akin to the ones observed by *M.tb* after exposure to human ALF, generate superior host immune responses and induce better protection against infection. Our studies highlight the importance of the properties of human ALF when developing an effective vaccine against TB.

RESULTS

***Vaccination with ALF-exposed BCG reduces bacterial burden in the lung and spleen of C57BL/6J and C3HeB/FeJ mice*.** To assess the efficacy of ALF-exposed BCG as a vaccine, C57BL/6J and C3HeB/FeJ (resistant and susceptible to TB, respectively[11, 12]) mice were vaccinated with either vehicle (mock-vaccinated; no BCG), NaCl- exposed BCG, or ALF-

exposed BCG. Six weeks after vaccination, all groups were infected with a low dose aerosol of ALF-exposed *M.tb* (the same ALF used for BCG exposure) to further mimic the *M.tb*-lung mucosa interactions within the lung. Mice were sacrificed at 14-days post infection (DPI) to assess early responses to *M.tb* infection (**Fig.1**), or at 250 DPI (C57BL/6J) or 100 DPI (C3HeB/FeJ), to assess long term control and signs of progressive disease[13]. Differences in timing were because C3HeB/FeJ mice have a median survival of 150 days[14].

At day 14-DPI, vaccination with ALF-BCG (black bars) resulted in a superior reduction in *M.tb* CFU in the lung beyond that afforded by NaCl-exposed BCG (grey bars), in both C57BL/6J (0.56-$\log_{10}$) and C3HeB/FeJ (0.24-$\log_{10}$) mice (**Fig.1A,C**). ALF-exposed BCG also conferred a better protection against dissemination in C57BL/6J mice (an additional 0.8-$\log_{10}$ protection), as indicated by a significant decrease in the bacterial burden in the spleen (**Fig.1A**). Though not significant, the same trend was also observed in C3HeB/FeJ mice (**Fig.1C**). Our data demonstrate that modification of BCG through exposure to ALF can further boost the protective efficacy of BCG *in vivo*, allowing for more rapid control of *M.tb* in the lung as demonstrated by significantly less *M.tb* CFU at 14-DPI.

At 250-DPI ALF-exposed BCG vaccination of C57BL/6J mice continued to confer superior protection (0.56-$\log_{10}$) compared to NaCl-exposed BCG vaccinated mice (0.25-$\log_{10}$), relative to vehicle control (**Fig.1B**). This trend was also found to be statistically significant in the spleen of C57BL/6J mice (**Fig.1B**), whereas C3HeB/FeJ mice showed superior long term control in the lung only (**Fig.1D**). Thus, vaccination with ALF-exposed BCG can enhance and extend the duration of protective immunity generated by BCG in the lung and spleen of C57BL/6J mice, and the lungs of C3HeB/FeJ mice. Overall, exposure of BCG to ALF prior to vaccination results in accelerated *M.tb* control (**Fig.1A,C**; early reduction in CFU) combined with the capacity to sustain control of *M.tb* for an extended period of time (**Fig.1B,D**; late reduction in CFU).

***Vaccination with ALF-exposed BCG attenuates immunopathology in the lung and extends survival*.** To determine the capacity of ALF-exposed BCG to reduce severity of infection and progression of disease, we assessed the degree of tissue inflammation through quantification of cellular aggregation relative to the total size of the lung. At 14-DPI (**Fig.2A,C**) C57BL/6J mice show no significant differences in tissue inflammation between the three groups studied (**Fig.2C**). However, mice vaccinated with ALF-exposed BCG appeared to have more perivascular and peribronchial lymphocytic cuffs compared to vehicle or NaCl- exposed BCG-vaccinated mice (**Fig.2A**), which suggests that the response to *M.tb* infection is accelerated in ALF-exposed BCG vaccinated mice. At 250-DPI, the lungs of vehicle- and NaCl-exposed BCG-vaccinated C57BL/6J mice contained abundant macrophages occupying a large proportion of the lung, while the lungs of ALF-exposed BCG vaccinated C57BL/6J mice had significantly reduced lung inflammation (**Fig.2A,D**). C3HeB/FeJ mice displayed similar phenotypes as C57BL/6J mice at 14-DPI with little inflammation observed in all three groups (**Fig.2B,E**) and at 100-DPI we again observed a significant decrease in the amount of infiltrating cells and lung inflammation in ALF-exposed BCG vaccinated mice *vs.* NaCl-exposed BCG vaccinated mice (**Fig.2B,F**). Importantly, compared to the vehicle, NaCl-exposed BCG vaccination showed extensive lung inflammation whereas vaccination with ALF-exposed BCG did not.

We determined the effectiveness of the ALF-exposed BCG vaccine to extend survival after *M.tb* infection. Vaccination with ALF-exposed BCG significantly extended the survival of C57BL/6J mice (**Fig.3**) to an average of 71 weeks, with some mice surviving ~80 weeks, demonstrating superior ability of ALF-exposed BCG to reduce TB severity. The mean survival of vehicle-treated mice was 50 weeks, which is in line with previously published data[13] and NaCl-exposed BCG vaccinated mice had a mean survival of 67.5 weeks. Altogether our data indicate that not only is vaccination with ALF-exposed BCG superior to NaCl-exposed BCG at reducing the bacterial burden in targeted organs and immunopathology of the lung, but it is also able to

extend survival of C57BL/6J mice. Despite observing decreased bacterial burden and immunopathology in ALF-exposed BCG vaccinated C3HeB/FeJ mice, we did not observe any extension in survival in this TB susceptible mouse strain (data not shown).

***Vaccination with ALF-exposed BCG enhances T-cell responses in the lung post M.tb challenge*.** Given that ALF-exposed BCG vaccination alone increased the number of activated $CD8^+$ T-cells in the lung (data not shown), and reduced the bacterial burden (**Fig.1**) and immuno-pathology in the lung (**Fig.2**) following *M.tb* challenge; we next sought to characterize T-cell responses in the lungs of vehicle, NaCl-, or ALF-exposed BCG vaccinated mice post *M.tb* challenge. C57BL/6J mice were vaccinated, challenged with *M.tb* via aerosol, and sacrificed at 14-DPI to characterize early T-cell responses in their lungs. The total number of $CD8^+$ T-cells in mice vaccinated with ALF-exposed BCG significantly increased compared to vehicle (as well as a trend for more *vs.* NaCl-exposed BCG), whereas the total number of $CD4^+$ T-cells did not differ between vaccination groups (**Fig.4A**).

We next characterized T-cell phenotypic and functional responses in vaccinated and *M.tb* challenged mice. Mice vaccinated with ALF-exposed BCG had significantly increased numbers of $CD8^+$ T-cells that expressed a memory phenotype and could secrete IFNγ, relative to both vehicle and NaCl-exposed BCG (**Fig.4B,E**). We also observed a significant increase in $CD44^+$ CD8 T-cells relative to NaCl-exposed BCG (**Fig.4D**). In contrast, CD69 expression was unchanged. Phenotypic and functional markers did not significantly differ for CD4 T-cells when comparing vehicle and ALF-exposed BCG (**Fig.4B-E**), although significance was observed between NaCl- and ALF-exposed BCG for CD69 (**Fig.4C**) and CD44 (**Fig.4D**) expression. Whole lung cells cultured with *M.tb* CFP showed an increased secretion of IFNγ, and decrease in secretion of IL-4 (data not shown), suggesting a shift towards T_h1 immunity in ALF-exposed

BCG vaccinated mice. These data indicate that, in contrast to NaCl-exposed BCG, vaccination with ALF-exposed BCG has a significant impact on CD8 T-cell numbers in the lung at day 14-DPI, and those cells expressed markers associated with a memory phenotype that has the capacity to secrete IFNγ. This phenotype was less apparent in the $CD4^+$ T-cell subset.

***$CD8^+$ T-cells in the lungs of ALF-exposed BCG vaccinated mice are required for enhanced protection against M.tb*.** Having observed significant increases in $CD8^+$ T-cell numbers and activity in the lung of ALF-exposed BCG vaccinated mice, we explored whether the reduction in bacterial burden observed in the lung of ALF-BCG vaccinated mice (**Fig.1**) was directly dependent on $CD8^+$ T-cells. Mice were vaccinated with vehicle, NaCl- or ALF-exposed BCG. Six weeks later, CD8 neutralizing antibodies or isotype controls were injected one day prior to *M.tb* infection and every four days thereafter. Mice were euthanized at 14-DPI to assess bacterial burden in the lung and spleen. Neutralizing antibodies successfully depleted $CD8^+$ T-cells from the lung without affecting the total number of $CD4^+$ T-cells (**Fig.5A,B**). Injection of isotype antibodies (**Fig.5C**) did not modify the vaccination efficacies that we previously demonstrated in **Fig.1**. $CD8^+$ T-cell depletion had no observable effect on *M.tb* burden in the lung and spleen of mice vaccinated with the vehicle control (**Fig.5C**), confirming that $CD8^+$ T-cells are not a major contributor at this stage of primary *M.tb* infection[15, 16]. Interestingly, $CD8^+$ T-cell depletion also had no effect on *M.tb* burden in the lung and spleen of mice that had received the NaCl-exposed BCG vaccination[17], though *M.tb* burden was still significantly reduced compared to vehicle-vaccinated mice (**Fig.5C**). However, in contrast to the NaCl-exposed BCG group, $CD8^+$ T-cell depletion of mice that has been vaccinated with ALF-exposed BCG lost the enhanced capacity to control *M.tb* infection (**Fig.5C**), restoring *M.tb* burden to that of NaCl-exposed BCG. These data indicate that activation and expansion of $CD8^+$ T-cells by ALF-exposed BCG is directly responsible for the enhanced protection induced by ALF-exposed BCG.

We also analyzed the levels of IFNγ and IL-12p40 in the lung of vaccinated and *M.tb* infected mice with or without $CD8^+$ T-cell depletion. Results showed significant increases in IFNγ in the lungs of mice vaccinated with both NaCl- and ALF-exposed BCG (**Fig.5D**), but the highest level of IFNγ was associated with ALF-exposed BCG vaccination. Similar to *M.tb* CFU, when ALF-BCG vaccinated mice were depleted of $CD8^+$ T-cells, IFNγ production in response to *M.tb* infection returned to levels comparable to NaCl-exposed BCG. These data identify $CD8^+$ T-cells and IFNγ as important contributors to the enhanced protection against *M.tb* challenge that is mediated by ALF-exposed BCG vaccination. We did not observe any differences in IL-12p40 between the vaccinated/$CD8^+$ T-cell depleted groups (**Fig.5D**), further supporting the concept that $CD8^+$ T-cells were a dominant source of IFNγ[18, 19] (and were not independently modifying Th1 responses that would lead to changes in IL-12p40). Though we did not extend our neutralization studies to later stages of the disease, we can postulate that the reduction in immunopathology observed at later time-points of *M.tb* infection (**Fig.2**) is directly linked to early (and potentially extended) $CD8^+$ T-cell activity in the lung.

DISCUSSION

Host immune responses to *M.tb* and the requirements for its control have been well studied[20], yet immune mechanisms that result in efficient *M.tb* clearance from the host remain unknown. Here we show that vaccination with ALF-exposed BCG is more efficacious at reducing *M.tb* bacterial burden in the lung and spleen early post infection (14-DPI), being superior to that of conventional (NaCl-exposed) BCG in both C57BL/6J and C3HeB/FeJ mouse strains, a resistant and a susceptible mouse model of TB research, respectively[11, 12]. Furthermore, at later stages of *M.tb* infection, mice vaccinated with ALF-exposed BCG retained a significantly lower bacterial burden in the lung and spleen compared to vehicle control, reduced immuno-pathology in the lung, and extended survival. Although we did not observe significant differences in bacterial

burden between NaCl- and ALF-exposed BCG vaccinated mice, trends for enhanced reduction in the ALF-exposed BCG group were evident. Our data support the concept that vaccine formulations capable of rapidly containing *M.tb* following infection are the most efficacious[21-23], where earlier control of *M.tb* infection can translate into a reduction in immunopathology and *M.tb* bacterial burden at later stages and extended survival. We extend on this concept by implementing a vaccine strategy that is directed against the phenotype of *M.tb* within the lung ALF, and demonstrate a clear enhancement of BCG protective efficacy.

We established that the ability of ALF-exposed BCG to control *M.tb* infection throughout the first 14 days was mediated by $CD8^+$ T-cells, with $CD8^+$ T-cell depletion reverting ALF-exposed BCG back to similar control as NaCl-exposed BCG. Furthermore ALF-exposed BCG vaccination led to increased numbers of activated ($CD69^+$) CD8 T-cells within the lung, and an increased number of memory phenotype and IFNγ secreting $CD8^+$ T-cells in the lungs after *M.tb* challenge. IFNγ levels in the lung were also reduced when $CD8^+$ T-cells were depleted. Thus, exposure of BCG to ALF resulted in a modified vaccine that could localize an increased number of activated $CD8^+$ T-cells to the lung post-vaccination. We anticipate that these cells matured to form a reservoir of memory $CD8^+$ T-cell could recognize and respond quickly upon encountering *M.tb.* This reservoir of memory $CD8^+$ T-cell could play a key role in protection as resident memory lymphocytes are critical for protective immune responses post BCG vaccination[24]. Furthermore, the reduction of bacterial burden in the lung and spleen of *M.tb*-infected mice receiving the ALF-exposed BCG vaccine was likely mediated by $CD8^+$ T-cell derived IFNγ as IFNγ concentration in the lung was directly dependent on the presence or absence of $CD8^+$ T-cells, despite similar numbers of $CD4^+$ T-cells in the lung. IFNγ is essential for the development of mycobacterial immunity[18, 25], and $CD8^+$ T-cell derived IFNγ has been previously shown to be important for protective immunity against *M.tb* infection[18, 19]. Why ALF-exposed BCG can better prime $CD8^+$

T-cells is unknown but we speculate that modifications to BCG cell wall motifs by ALF, as we showed for *M.tb*[8], may alter uptake pathways by phagocytes[7, 26] or enhance antigen cross-presentation of antigens that are presented during *M.tb* infection in the lung via mechanisms such as apoptosis[27] and/or autophagy[28]. Induction of these pathways has been shown to be effective methods of enhancing BCG efficacy[29-31].

The functionality of $CD8^+$ T-cell in BCG vaccination has not been extensively addressed[32]. Recent studies show that administration of BCG into the mouse lungs generates protective CD8 T cell resident memory cells [33]. Here we observed a similar phenotype but by subcutaneous administration of ALF-exposed BCG, which at the same time reduced lung tissue damage. The mechanism(s) behind how $CD8^+$ T-cells contribute to the efficacy of ALF-exposed BCG could be through their cytotoxic function[34-36], their ability to stimulate other cells via secretion of specific immunomodulators[36], and/or their ability to induce apoptosis of cells via the FasL-Fas pathways targeting cells expressing Fas[30]. Any of these mechanisms could lead to the early *M.tb* control we observe, and we can also speculate that they contribute to the extended control of *M.tb* infection and reduced immuno-pathology that are observed as $CD8^+$ T-cells have typically been associated with containment of *M.tb* infection[37].

In addition to altering early immune events in the lung, ALF-exposed BCG vaccination reduced manifestations of disease (*i.e.* inflammation of the lung). Interestingly, *M.tb* infected C57BL/6J mice that received the ALF-exposed BCG vaccine experienced similar levels of inflammation early in the lung compared to non-vaccinated mice or mice vaccinated with the conventional BCG. However, at 250-DPI a 57% reduction in tissue damage was observed in the C57BL/6J mice vaccinated with ALF-exposed BCG when compared to vehicle. In this regard, conventional BCG vaccination only reduced inflammation by 19.5% in this mouse strain. Further, in the TB susceptible C3HeB/FeJ mouse model, conventional BCG vaccination tended to exacerbate lung

inflammation, whereas the ALF-exposed BCG vaccine reduced inflammation to less than 10% area of the lungs covered by inflammation. It is feasible that the early recruitment of IFNγ^+ CD8$^+$ T-cells induced by ALF-exposed BCG vaccination at 14-DPI may have simply reduced *M.tb* infection to low enough levels to induce less inflammation, but equally plausible that long term control may have been a more active process. The reduced inflammation in ALF-exposed BCG vaccinated mice did not correlate with the levels of cytokines present in the lung during *M.tb* infection, as no differences in the levels of TNF, IL-10, IL-12p40 and IFNγ in lung homogenates of NaCl- and ALF-exposed BCG vaccinated mice were noted at day 14- and 250-DPI (data not shown). However, in both NaCl- and ALF-exposed BCG vaccinated mice, the levels of IL-12p40 and IFNγ were significantly higher than the vehicle at 14-DPI (data not shown), indicating a strong Th1 response being generated in vaccinated animals.

Our vaccination model also shows that exposure to ALF enhances the efficacy of BCG not only in terms of reducing bacterial burden in target organs and reducing immuno-pathology, but in its ability to increase the survival of vaccinated mice. C57BL/6J mice vaccinated with ALF-exposed BCG had a significantly longer lifespan compared to NaCl-exposed BCG vaccinated mice. Consistent with previously published data[38], we observed lower bacterial burden and reduced immunopathology in BCG vaccinated C3HeB/FeJ mice; but we did not observe the same survival trend in C3HeB/FeJ mice as C57BL/6J mice (data not shown). In the C3HeB/FeJ mouse model, neither NaCl- nor ALF-exposed BCG were effective at extending survival after *M.tb* infection, suggesting that this mouse model might present limitations for testing the efficacy of new TB vaccines. Though similar experiments have been conducted to evaluate the efficacy of BCG in C3HeB/FeJ mice[39], the route of vaccination and infection differed from ours [intravenous BCG vaccination and intravenous *M.tb* infection[39] *vs.* subcutaneous BCG vaccination and *M.tb* aerosol infection (ours)], suggesting that the route of

immunization/infection is important in the context of disease outcome[3]. Additionally, the rapid onset of TB disease in C3HeB/FeJ mice compared to C57BL/6J mice might explain the differences in survival[40].

The fact that exposure to ALF was able to increase the efficacy of BCG vaccination in terms of reducing bacterial burden and improving immunopathology suggests that manipulation of BCG, particularly with emphasis on its cell wall composition at the time of vaccination, offers novel avenues to understand and improve on the development of protective immunity to mycobacteria. Understanding the changes brought forth to BCG by the action of ALF, particularly in the context of exploiting the biochemical properties of the mycobacterial cell wall, can lead to the development of more efficacious vaccines against TB.

MATERIALS AND METHODS

Ethics statement. This study was carried out in strict accordance with US Code of Federal and Local (University IRB) Regulations, and Good Clinical Practice as approved by the National Institutes of Health (NIAID/DMID branch).

Mice. Specific- pathogen-free, female mice aged 6-8 weeks of the C57BL/6J or C3HeB/FeJ background were purchased from Jackson Laboratories (Bar Harbor, ME). Upon arrival, mice were supplied with sterilized water and chow *ad libitum* and acclimatized for at least one week prior to experimental manipulation. Mice were maintained in micro-isolator cages located in either a standard vivarium for all noninfectious studies or in a biosafety level three (ABSL-3) core facilities for all studies involving *M.tb*. Mice were divided into three groups: Mock-vaccinated (vehicle), NaCl-exposed BCG-vaccinated, or ALF-exposed BCG-vaccinated. All experimental procedures were approved by The Ohio State University Institutional Laboratory Animal Care and Use Committee.

Growth conditions of M.tb and M. bovis BCG strain Pasteur*.* GFP-*M.tb* Erdman (provided by Dr. Horwitz, UCLA, CA) and *M. bovis* BCG Pasteur strains [American Type Culture Collection (ATCC), #35734] were grown as previously described[41].

Collection of human ALF and exposure to bacteria*.* Human ALF was obtained was obtained from human bronchoalveolar lavage fluid (BALF), concentrated to its physiological concentration within the human lung as we previously described[8-10], and stored at -80°C until use. Single cell suspensions of *M.tb* or *M. bovis* BCG were exposed to ALF for 12h at 37°C, 5% CO_2. Bacteria were then washed extensively with 0.9%NaCl to remove ALF and suspended at working concentrations for aerosol infections or subcutaneous injections with *M.tb* or *M. bovis* BCG, respectively.

Vaccination*.* Mice were subcutaneously injected in the scruff of the neck with 100 μl of 0.9%NaCl (saline, vehicle), 0.9%NaCl-exposed, or ALF-exposed *M. bovis* BCG Pasteur (7.5×10^5 CFU), diluted in sterile 0.9%NaCl. Mice were housed without further experimental manipulation for six weeks.

M.tb aerosol infection and colony forming unit enumeration*.* Mice were infected aerogenically with a low dose of *M.tb* using the Glas-Col (Terre Haute, IN) inhalation exposure system as previously described[42]. Bacterial burden was assessed at various DPI by culturing serial dilutions of organ homogenates onto Middlebrook 7H11 agar supplemented with OADC as we have previously described[42]. Colonies were enumerated following 14-21 days incubation at 37°C. Data are expressed as the $\log_{10}$ value of the mean number of CFU recovered per organ (n=4–5 mice). Lung homogenate were also plated onto OADC supplemented 7H11 agar

containing 2 μg/ml of 2-thiophenecarboxylic acid hydrazide (TCH; Sigma-Aldrich) to exclude and differentiate BCG growth from *M.tb*[43]

Lung cell isolation. Lung cells were isolated as previously described[44]. Briefly, mice were sacrificed, and the lungs were cleared of blood via perfusion through the pulmonary artery with 10 ml PBS containing 50 U/ml heparin and placed into 2 ml cold complete-DMEM (c-DMEM) [DMEM (Mediatech, Herndon, VA), supplemented with 10% heat-inactivated FBS (Atlas Biologicals, Ft. Collins, CO), 1% HEPES buffer (1 M, Sigma-Aldrich), 10 ml 100x nonessential amino acid solution (Sigma-Aldrich), 5 ml penicillin/streptomycin solution (50,000 U penicillin, 50 mg streptomycin, Sigma-Aldrich), and 0.1% 2-Mercaptoethanol (50 mM, Sigma-Aldrich)]. The lungs were then supplemented with 2 ml c-DMEM containing collagenase XI and type IV bovine pancreatic DNase, before being partially dissociated using the mouse lung dissociator program one on the gentleMACS tissue dissociator (Miltenyi Biotec). The tissue was then incubated for 30 min at 37°C, 5%CO_2. After incubation, the tissue was further dissociated by using program two on the gentleMACS dissociator. Digested lungs were dispersed gently through a 70 μm nylon screen to obtain a single-cell suspension. Residual RBCs were lysed using Gey's lysis buffer, and washed with c-DMEM. Cell suspensions were counted using trypan blue to exclude dead cells and suspended at a working concentration in c-DMEM or fixed for flow cytometry as described below.

Immunophenotyping by flow cytometry. Lung cell were prepared for flow cytometry as previously described[44]. Briefly, cell suspensions were adjusted to $1x10^7$ cells/ml in d-RPMI buffer and incubated at 4°C for one hour. Cells ($1×10^6$) were labeled with 25 μg/ml of specific fluorescent-labeled antibody for 30 min at 4°C in the dark then washed. For intracellular staining $5x10^6$ cells were first stimulated with 10 μg/ml CD3ε, 1 μg/ml of CD28 and 3 μM of monensin for

4h at 37°C, 5%CO_2[42]. Cells were then labeled with cell surface markers, permeabilized using BD Cytofix/Cytoperm™ Plus and then labeled with intracellular markers as directed by manufacturer for 30 min at 4°C in the dark. Samples were read on a Becton Dickinson LSRII flow cytometer (in BSL3 facility) or FACSCanto II, and data were analyzed using FlowJo version 10 software. Lymphocytes were gated according to their forward- and side-scatter profiles, and CD4 or CD8 T-cells were identified by the presence of specific, fluorescent-labeled antibody in combination with CD3ε. Cell surface markers analyzed were: FITC-conjugated CD8 (5H10-1-BioLegend), PE-conjugated CD69 (H1.2F3-BD Biosciences), PE-conjugated CD197/CCR7 (4B12-BD Biosciences), PerCP-Cy5.5-conjugated CD44 (IM7-BD Biosciences), PerCP-Cy5.5-conjugated CD3 (145-2C11-BD Biosciences), APC-conjugated IFNγ (XMG1.2-BD Biosciences), APC-conjugated CD62L (MEL-14-BD Biosciences), PE-Cy7-conjuated CD8 (53-6.7-BD Biosciences), and APC-Cy7-conjugated CD4 (GK1.5-BD Biosciences). Appropriate isotype controls recommended by the manufacturer were included in each experiment and used to set gates for analysis.

Cell stimulation and ELISA. Stimulation of cells was performed as described[45]. Briefly, lung cell preparations in c-DMEM were counted and $1x10^6$ cells plated per well in a 96-well flat plate. Lung cells were incubated with 10 μg/ml ovalbumin (OVA) as a negative control, 10 μg/ml *M.tb* $H_{37}R_v$ CFP, or 10 μg/ml of the mitogen concacavalin A as a positive control at 37°C, 5%CO_2 for 72 h. Following the incubation period, supernatants were analyzed for levels of IFNγ and IL-4 by ELISA following manufacturer's instructions (BD OptEIA). ELISAs were read on a Spectramax M2 Microplate reader (Molecular Devices LLC, Sunnyvale, California).To assess proliferation, lung cells were incubated with the conditions described above in the presence of CFSE (CellTrace, ThermoFisher Scientific) at 37°C, 5%CO_2 for 7h, fixed and then stained for flow cytometry.

Cell depletion. Cells depletions were performed as previously described[46]. Briefly, 500 μg anti-$CD8^+$ (Clone: 53.6.72) depletion antibody (BioXCell, West Lebanon, NH) or whole rat IgG2a (Clone: 2A3) (BioXCell) in 100 μl were injected into the intraperitoneal cavity four times over a period of two weeks beginning one day prior to *M.tb* challenge. Lungs were digested to obtain whole lung cells and stained with fluorophore conjugated antibodies for flow cytometry analysis to confirm CD8 T-cell depletion.

Histopathology*.* The middle right lung was isolated from each individual mouse and inflated with and stored in 10% neutral buffered formalin (NBF). Lung tissue was processed, sectioned, and stained with Hematoxylin and eosin for light microscopy with lobe orientation designed to allow for maximum surface area of each lobe to be seen. Sections were examined by a board-certified veterinary pathologist without prior knowledge of the experimental groups and evaluated for according to severity, granuloma size and number, cellular composition, lymphocytic cuffing, and necrosis. Areas of cell aggregation (inflammation) were quantified using Aperio Imagescope at 4x magnification by calculating the total area of the inflamed tissue over the total area of the lobe for each individual mouse.

Statistical analysis*.* Statistical significance was determined using Prism 4 software (GraphPad Software, San Diego, CA). The unpaired, two-tailed Student's t-test was used for two group comparisons. Multiple comparisons were analyzed using one-way ANOVA with Tukey's post-test. Log-Rank test was used to determine statistical significance of survival experiments. Statistical significance was reported as *$p<0.05$; **$p<0.01$; or ***$p<0.001$.

DISCLOSURE/CONFLICT OF INTEREST

Authors declare no conflict of interest.

ACKNOWLEDGEMENTS

We thank Drs. Larry S. Schlesinger and Jian Zhang for their careful review of this manuscript. This work was supported by the National Institute of Allergy and Infectious Diseases at the National Institutes of Health (NIH/NIAID), grant numbers [AI073856 and AI093570] to JBT; by the National Institute on Aging at the National Institute of Health [AG051428] supporting JT and JBT; and by The Ohio State University College of Medicine Systems in Integrative Biology Training Program - NIH/NIGMS T32-GM068412 and NIH/NIAID AI093570-S1 partially supporting JIM. This study was also partially supported by a CTSA award No UL1TR001070 from the National Center for Advancing Translational Sciences. We thank the University Laboratory Animal Resources and personnel and the Comparative Pathology & Mouse Phenotyping Shared Resource, Department of Veterinary Biosciences and the Comprehensive Cancer Center, The Ohio State University, Columbus, OH, supported in part by grant P30 CA016058, National Cancer Institute, Bethesda, MD provided digital slide scanning services using Aperio ScanScope. We would like to acknowledge the facilities and programmatic support of the OSU Biosafety Level 3 Program.

FIGURES

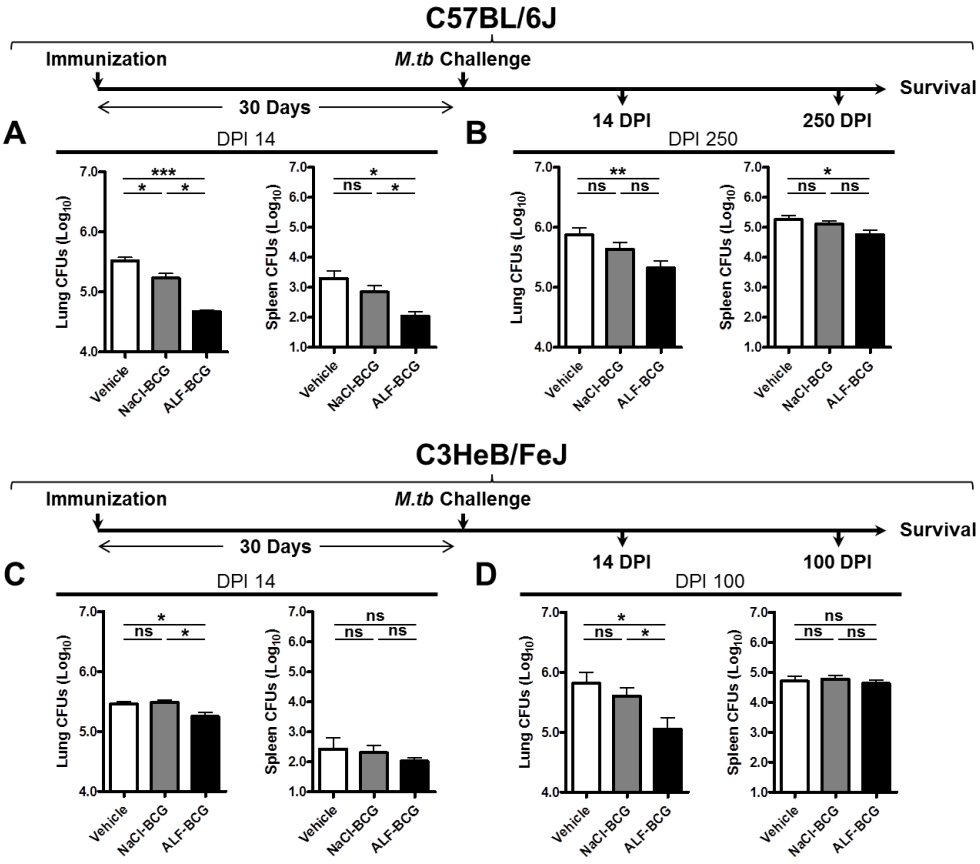

Figure 1. *M.tb* bacterial burden in the lung and spleen of C57BL/6J and C3HeB/FeJ mouse strains. C57BL/6J and C3HeB/FeJ mice were vaccinated with NaCl-exposed BCG (NaCl-BCG; grey bars) or ALF-exposed BCG (ALF-BCG; black bars), or left unvaccinated (vehicle; open bars). Six weeks later, mice were infected with a low dose aerosol of *M.tb*. C57BL/6J mice (**A, B**) were sacrificed at 14 and 250 days post infection and *M.tb* CFU determined in lung and spleen. Representative experiments from n=3 with 4-5 mice per group per time-point studied, mean ± SEM; one-way ANOVA with Tukey's post-hoc test, **p*<0.05, ***p*<0.01, ****p*<0.001. C3HeB/FeJ mice (**C, D**) were sacrificed at 14 and 100 days post infection and *M.tb* CFU determined in lung and spleen. Data from one experiment with 5 mice per group per time-point, mean ± SEM; **p*<0.05; ns: not significant.

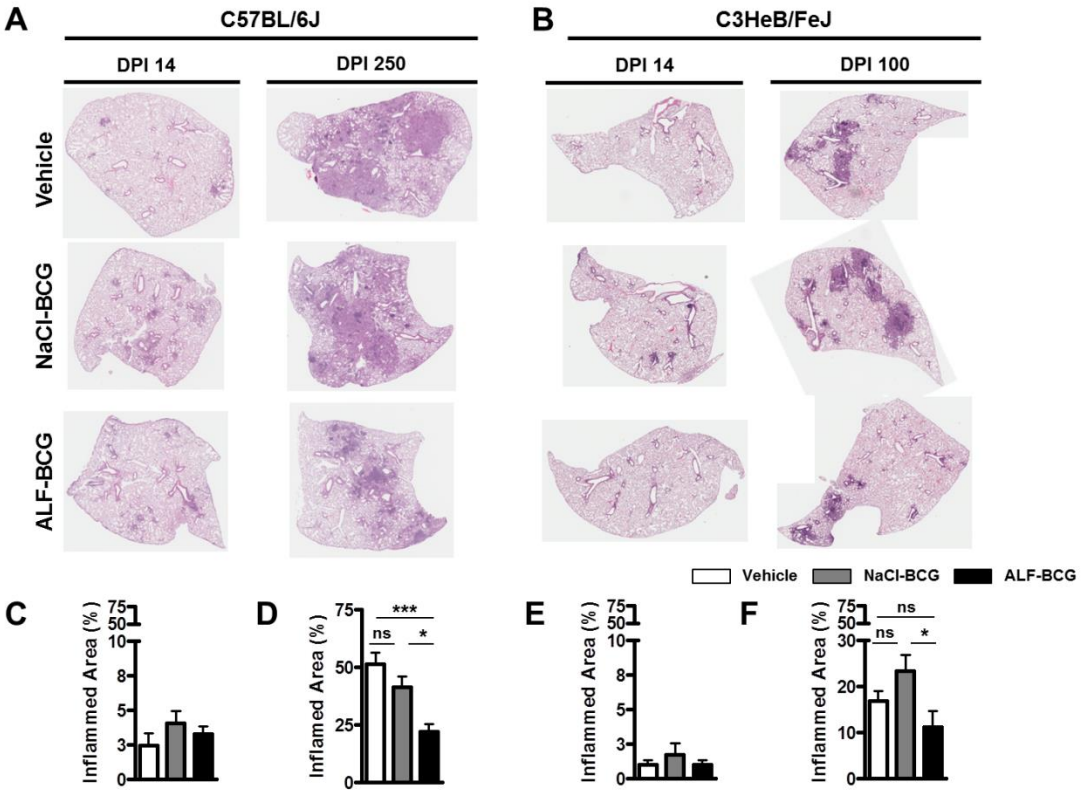

Figure 2. Immunohistopathology of *M.tb* infected lung in vaccinated mice. C57BL/6J (**A, C, D**) and C3HeB/FeJ (**B, F, G**) mice were vaccinated with NaCl-exposed BCG (NaCl-BCG; grey bars) or ALF-exposed BCG (ALF-BCG; black bars), or left unvaccinated (vehicle; open bars). Six weeks later, mice were infected with a low dose aerosol of *M.tb*. At 14 and 250 DPI for C57BL/6J or 14 and 100 DPI for C3HeB/FeJ, mice were sacrificed and lungs fixed in 10% NBF, embedded in paraffin, sectioned, and stained with hematoxylin and eosin to visualize tissue morphology. Areas of cell aggregation (inflammation) were quantified using Aperio Imagescope. For C57BL/6J mice, a representative experiment from n=3 with 4-5 mice per group per time-point, mean ± SEM; one-way ANOVA with Tukey's post-hoc test, *p<0.05, ***p<0.001. For C3HeB/FeJ data are from one experiment with 5 mice per group per time-point, mean ± SEM; one-way ANOVA with Tukey's post-hoc test *p<0.05; ns: not significant.

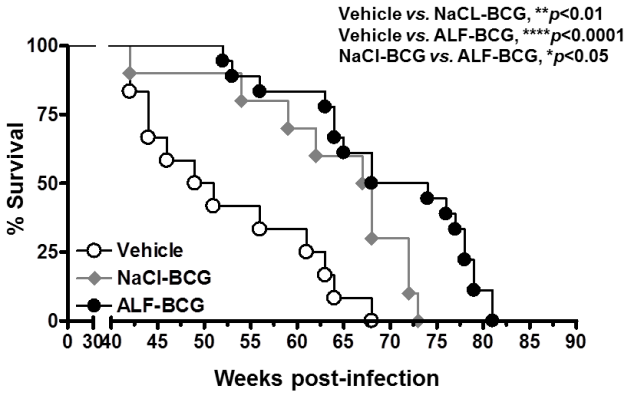

Figure 3. Vaccination with ALF-BCG extends survival of C57BL/6J mice. C57BL/6J mice were vaccinated with vehicle (open circles), NaCl-exposed BCG (grey diamonds) or ALF-exposed BCG (black circles) and challenged with *M.tb* six weeks later. Survival was monitored across a period of 85 weeks. Mice were euthanized when they met the exclusion criteria documented in animal care and use protocols, and the date documented. Mice receiving vehicle displayed a mean survival of 50.00 weeks. NaCl-BCG vaccinated mice had a mean survival of 67.50 weeks. ALF-BCG vaccinated mice had a mean survival of 71.00 weeks. Pooled experiment from n=3 with 15-20 mice, mean ± SEM; Log-rank test, **Vehicle *vs.* NaCl-BCG (p=0.0097), ****Vehicle *vs.* ALF-BCG (p<0.0001), *NaCl-BCG *vs.* ALF-BCG (p=0.0307).

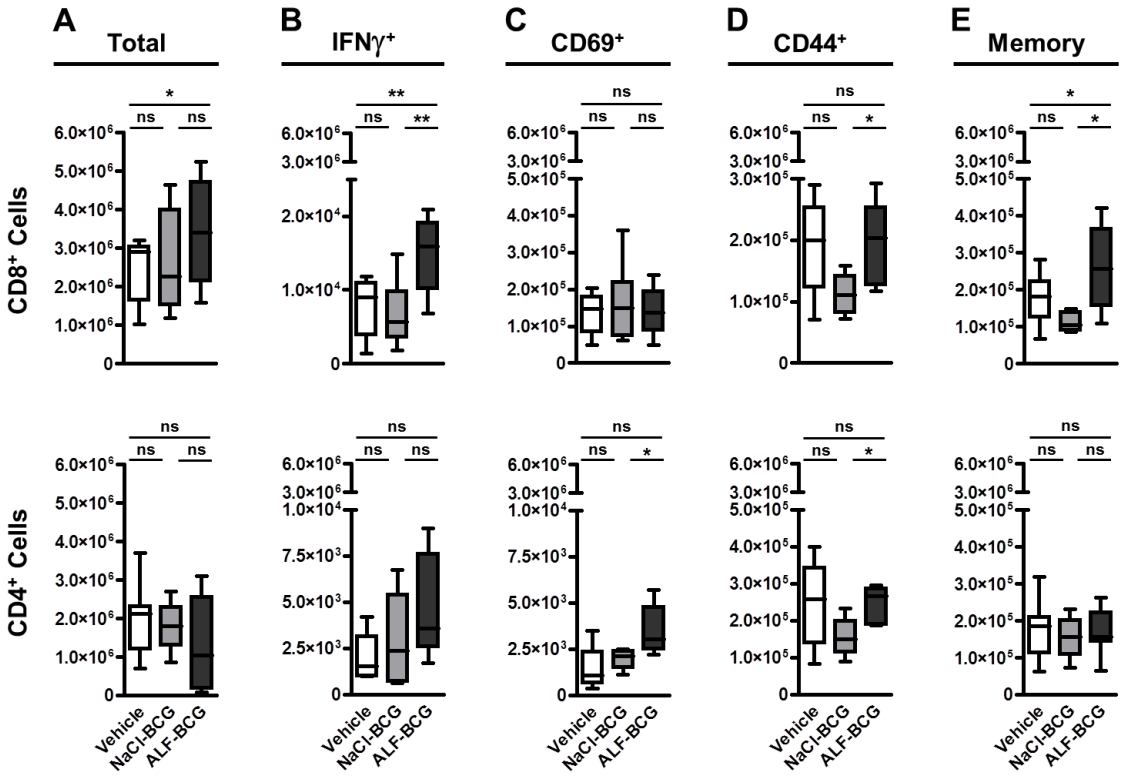

Figure 4. T-cell responses in lung of vaccinated mice infected with *M.tb* at 14 DPI. C57BL/6J were vaccinated with vehicle (open bars), NaCl-exposed BCG (grey bars), or ALF-exposed BCG (black bars). Six weeks post vaccination; mice were challenged with *M.tb* and euthanized at 14 DPI to characterize immune cell populations in the lung by flow cytometry. (**A**) Total number of $CD4^+$ and $CD8^+$ T-cells in the lung. (**B**) Lung cells were stimulated CD3/CD28 in the presence of monensin for 4 hours and stain for cell surface markers and intracellular IFNγ. (**C**) Total number of $CD8^+$ $CD69^+$ and $CD4^+CD69^+$ T-cells (**D**) Total number of $CD8^+CD44^+$ and $CD4^+CD44^+$ T-cells. (**E**) Total number $CD8^+$ $CD62L^+CCR7^-$ $CD44^+$ and $CD4^+CD62L^+CCR7^-$ $CD44^+$ effector memory T-cells. Pooled experiment from n=2 with 5 mice per group, mean ± SEM; one-way ANOVA with Tukey's post-hoc test, *p<0.05, **p<0.01; ns: not significant.

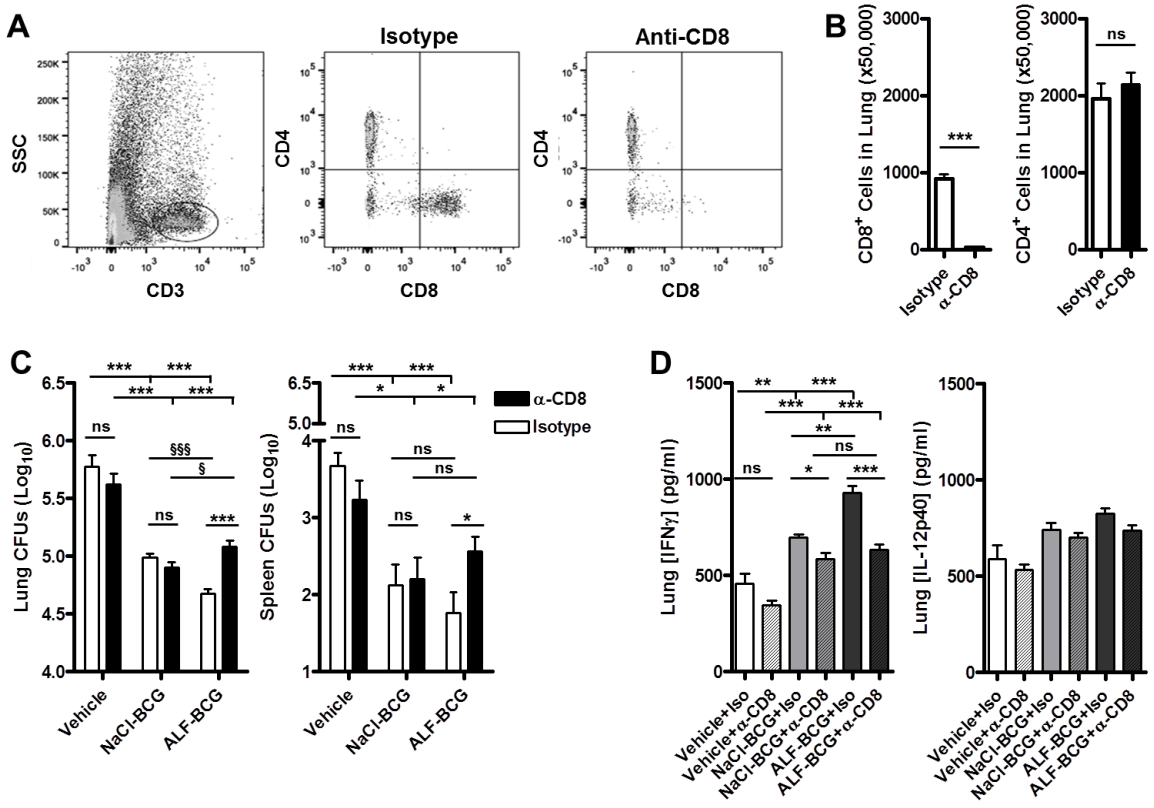

Figure 5. **Reduction in bacterial burden associated with ALF-BCG is dependent on CD8$^+$ T-cell responses.** C57BL/6J mice were vaccinated with vehicle, NaCl-exposed BCG, or ALF-exposed BCG. Six weeks after vaccination, mice were i.p. injected with 500μg of anti-CD8a, or rat IgG2a and challenged with *M.tb.* Anti-CD8a or rat IgG2a was delivered 1 day prior to *M.tb* challenge and every 4 days thereafter. Mice were sacrificed at 14 DPI. (**A**) Schematic depicting effective depletion of CD8$^+$ T-cells from the lung. (**B**) Quantification of CD8$^+$ and CD4$^+$ T-cells in the lung of isotype-injected or anti-CD8 injected mice. CD8$^+$ T-cells were depleted to less than 20 cells per 50,000 cells. Depletion of CD8$^+$ T-cells did not affect the number of CD4$^+$ T-cells in the lung. Pooled experiment from n=2 with 5 mice/per group, mean ± SEM; student's-t test, ***p<0.001. (**C**) *M.tb* CFU were determined in the lung and spleen at 14 DPI. Pooled experiment from n=2 with 5 mice/per group, mean ± SEM; one-way ANOVA with Tukey's post-hoc test or student's *t*-test (for single comparisons), *p<0.05, **p<0.01, ***p<0.001, $^{§}p$<0.05, $^{§§§}p$<0.01; ns:

not significant. (**D**) IFNγ and IL-12p40 in the lung homogenates of vehicle-treated or vaccinated mice with or without $CD8^+$ T-cells depletion at 14 DPI. Pooled experiment from n=2 with 5 mice/per group, mean ± SEM, one-way ANOVA with Tukey's post-hoc test (for multiple groups) or student's t-test (for single comparisons), *p<0.05, **p<0.01, ***p<0.001.

REFERENCES

1. World Health Organization. Global Tuberculosis Report 2016. 2016. http://apps.who.int/iris/bitstream/10665/250441/1/9789241565394-eng.pdf?ua=1

2. Smith,K.C., Orme,I.M., & Starke,J.R. Tuberculosis vaccines in *Vaccines* 789-811 (Saunders, 2012).

3. Moliva,J.I., Turner,J., & Torrelles,J.B. Prospects in *Mycobacterium bovis* Bacille Calmette et Guerin (BCG) vaccine diversity and delivery: Why does BCG fail to protect against tuberculosis? *Vaccine* **33**, 5035-5041 (2015).

4. Abubakar,I. *et al.* Systematic review and meta-analysis of the current evidence on the duration of protection by bacillus Calmette-Guerin vaccination against tuberculosis. *Health Technol. Assess.* **17**, 1-vi (2013).

5. Smith,I. Mycobacterium tuberculosis pathogenesis and molecular determinants of virulence. *Clin. Microbiol. Rev.* **16**, 463-496 (2003).

6. Whitsett,J.A., Wert,S.E., & Weaver,T.E. Alveolar surfactant homeostasis and the pathogenesis of pulmonary disease. *Annu. Rev. Med.* **61**, 105-119 (2010).

7. Sasindran,J. & Torrelles JB *Mycobacterium tuberculosis* infection and inflammation: What is beneficial for the host and for the bacterium? *Front. Microbiol.* **2**, 1-16 (2011).

8. Arcos,J. *et al.* Human lung hydrolases delineate *Mycobacterium tuberculosis*-macrophage interactions and the capacity to control infection. *J. Immunol.* **187**, 372-381 (2011).

9. Arcos,J. *et al.* Lung mucosa lining fluid modifies *Mycobacterium tuberculosis* to reprogram human neutrophil killing mechanisms . *J. Infect. Dis.* **212**, 948-958 (2015).

10. Arcos,J. *et al. Mycobacterium tuberculosis* cell wall released fragments by the action of the human lung mucosa modulate macrophages to control infection in an IL-10-dependent manner. *Mucosal Immunol.*(2016) [ePub ahead of print].

11. Driver,E.R. *et al.* Evaluation of a mouse model of necrotic granuloma formation using C3HeB/FeJ mice for testing of drugs against *Mycobacterium tuberculosis*. *Antimicrob. Agents Chemother.* **56**, 3181-3195 (2012).

12. Medina,E. & North,R.J. Resistance ranking of some common inbred mouse strains to *Mycobacterium tuberculosis* and relationship to major histocompatibility complex haplotype and Nramp1 genotype. *Immunology* **93**, 270-274 (1998).

13. Cyktor,J.C. *et al.* KLRG1 deficiency significantly enhances survival after *Mycobacterium tuberculosis* infection. *Infect. Immun.* **81**, 1090-1099 (2013).

14. Lanoix,J.P., Lenaerts,A.J., & Nuermberger,E.L. Heterogeneous disease progression and treatment response in a C3HeB/FeJ mouse model of tuberculosis. *Dis Model. Mech.* **8**, 603-610 (2015).

15. Turner,J. *et al.* CD8- and CD95/95L-dependent mechanisms of resistance in mice with chronic pulmonary tuberculosis. *Am. J. Respir. Cell Mol. Biol.* **24**, 203-209 (2001).

16. Xing,Z., Wang,J., Croitoru,K., & Wakeham,J. Protection by CD4 or CD8 T cells against pulmonary *Mycobacterium bovis* bacillus Calmette-Guerin infection. *Infect. Immun.* **66**, 5537-5542 (1998).

17. Chen,C.Y. *et al.* A critical role for CD8 T cells in a nonhuman primate model of tuberculosis. *PLoS. Pathog.* **5**, e1000392 (2009).

18. Tascon,R.E., Stavropoulos,E., Lukacs,K.V., & Colston,M.J. Protection against *Mycobacterium tuberculosis* infection by CD8+ T cells requires the production of gamma interferon. *Infect. Immun.* **66**, 830-834 (1998).

19. Serbina,N.V. & Flynn,J.L. Early emergence of CD8(+) T cells primed for production of type 1 cytokines in the lungs of *Mycobacterium tuberculosis*-infected mice. *Infect. Immun.* **67**, 3980-3988 (1999).

20. Flynn,J.L. & Chan,J. Immunology of tuberculosis. *Annu. Rev. Immunol.* **19**, 93-129 (2001).

21. Ordway,D. *et al.* Influence of *Mycobacterium bovis* BCG vaccination on cellular immune response of guinea pigs challenged with *Mycobacterium tuberculosis*. *Clin. Vaccine Immunol.* **15**, 1248-1258 (2008).

22. Santosuosso,M. *et al.* Mucosal luminal manipulation of T cell geography switches on protective efficacy by otherwise ineffective parenteral genetic immunization. *J. Immunol.* **178**, 2387-2395 (2007).

23. Khader,S.A. *et al.* IL-23 and IL-17 in the establishment of protective pulmonary CD4+ T cell responses after vaccination and during *Mycobacterium tuberculosis* challenge. *Nat. Immunol.* **8**, 369-377 (2007).

24. Connor,L.M. *et al.* A key role for lung-resident memory lymphocytes in protective immune responses after BCG vaccination. *Eur. J. Immunol.* **40**, 2482-2492 (2010).

25. Ladel,C.H., Daugelat,S., & Kaufmann,S.H.E. Immune response to *Mycobacterium bovis* bacille Calmette Guérin infection in major histocompatibility complex class I- and II-deficient knock-out mice: Contribution of CD4 and CD8 T cells to acquired resistance. *Eur. J. Immunol.* **25**, 377-384 (1995).

26. Ferguson,J.S. *et al.* Surfactant protein D increases fusion of *Mycobacterium tuberculosis*-containing phagosomes with lysosomes in human macrophages. *Infect. Immun.* **74**, 7005-7009 (2006).

27. Karakousis,P.C., Bishai,W.R., & Dorman,S.E. *Mycobacterium tuberculosis* cell envelope lipids and the host immune response. *Cell. Microbiol.* **6**, 105-116 (2004).

28. Winau,F. *et al.* Apoptotic vesicles crossprime CD8 T cells and protect against tuberculosis. *Immunity* **24**, 105-117 (2006).

29. Woodworth,J.S., Wu,Y., & Behar,S.M. *Mycobacterium tuberculosis*-specific CD8+ T cells require perforin to kill target cells and provide protection *in vivo*. *J. Immunol.* **181**, 8595-8603 (2008).

30. Oddo,M. *et al.* Fas ligand-induced apoptosis of infected human macrophages reduces the viability of intracellular *Mycobacterium tuberculosis*. *J. Immunol.* **160**, 5448-5454 (1998).

31. Jagannath,C. *et al.* Autophagy enhances the efficacy of BCG vaccine by increasing peptide presentation in mouse dendritic cells. *Nat. Med.* **15**, 267-276 (2009).

32. Abebe,F. Is interferon-gamma the right marker for bacille Calmette-Guerin-induced immune protection? The missing link in our understanding of tuberculosis immunology. *Clin. Exp. Immunol.* **169**, 213-219 (2012).

33. Perdomo,C. *et al.* Mucosal BCG vaccination induces protective lung-resident memory T cell populations against tuberculosis. *MBio* **7**, pii: e01686-16 (2016).

34. Turner,J. & Dockrell,H.M. Stimulation of human peripheral blood mononuclear cells with live *Mycobacterium bovis* BCG activates cytolytic CD8+ T cells *in vitro*. *Immunology* **87**, 339-342 (1996).

35. Murray,R.A. *et al.* Bacillus Calmette Guerin vaccination of human newborns induces a specific, functional CD8+ T cell response. *J. Immunol.* **177**, 5647-5651 (2006).

36. Bevan,M.J. Helping the CD8(+) T-cell response. *Nat. Rev. Immunol.* **4**, 595-602 (2004).

37. van Pinxteren,L.A., Cassidy,J.P., Smedegaard,B.H., Agger,E.M., & Andersen,P. Control of latent *Mycobacterium tuberculosis* infection is dependent on CD8 T cells. *Eur. J. Immunol.* **30**, 3689-3698 (2000).

38. Henao-Tamayo,M. *et al.* Differential *Mycobacterium bovis* BCG vaccine-derived efficacy in C3Heb/FeJ and C3H/HeOuJ mice exposed to a clinical strain of Mycobacterium tuberculosis. *Clin. Vaccine Immunol.* **22**, 91-98 (2015).

39. Yan,B.S. *et al.* Progression of pulmonary tuberculosis and efficiency of bacillus Calmette-Guerin vaccination are genetically controlled via a common sst1-mediated mechanism of innate immunity. *J. Immunol.* **179**, 6919-6932 (2007).

40. Pan,H. *et al. Ipr1* gene mediates innate immunity to tuberculosis. *Nature* **434**, 767-772 (2005).

41. Torrelles,J.B. *et al.* Identification of *Mycobacterium tuberculosis* clinical isolates with altered phagocytosis by human macrophages due to a truncated lipoarabinomannan. *J. Biol. Chem.* **283**, 31417-31428 (2008).

42. Cyktor,J.C. *et al.* IL-10 Inhibits Mature Fibrotic Granuloma Formation during *Mycobacterium tuberculosis* Infection. *J. Immunol.* **190**, 2778-2790 (2013).

43. Flaherty,D.K., Vesosky,B., Beamer,G.L., Stromberg,P., & Turner,J. Exposure to *Mycobacterium avium* can modulate established immunity against *Mycobacterium tuberculosis* infection generated by *Mycobacterium bovis* BCG vaccination. *J. Leukoc. Biol.* **80**, 1262-1271 (2006).

44. Canan,C.H. *et al.* Characterization of lung inflammation and its impact on macrophage function in aging. *J. Leukoc. Biol.* **96**, 473-480 (2014).

45. Beamer,G.L., Flaherty,D.K., Vesosky,B., & Turner,J. Peripheral blood gamma interferon release assays predict lung responses and *Mycobacterium tuberculosis* disease outcome in mice. *Clin. Vaccine Immunol.* **15**, 474-483 (2008).

46. Cyktor,J.C., Carruthers,B., Beamer,G.L., & Turner,J. Clonal Expansions of CD8(+) T Cells with IL-10 Secreting Capacity Occur during Chronic *Mycobacterium tuberculosis* Infection. *PLoS ONE* **8**, e58612 (2013).